RAPID COMMUNICATIONS

PHYSICAL REVIEW B VOLUME 51, NUMBER 14 1 APRIL 1995-II

Photon-activated switch behavior in the single-electron transistor with a superconducting island

J. M. Hergenrother, J. G. Lu, M. T. Tuominen,* D. C. Ralph, and M. Tinkham
Division of Applied Sciences and Department of Physics, Harvard University, Cambridge, Massachusetts 02138
(Received 13 February 1995)

We show that the effects of photon-assisted tunneling in the single-electron transistor are dramatically enhanced if the mesoscopic island is superconducting. Many electrons can tunnel through the system for each absorbed photon as a result of an even-odd electron number effect in the superconducting island. For suitable bias, the device acts as a photon-activated switch from a low- to a high-current state, providing a sensitive mechanism for microwave detection. A simple model quantitatively describes this particular consequence and other less dramatic effects of microwave radiation.

The single-electron tunneling (SET) transistor with a superconducting island is an ideal system for studying single-charge transport and even-odd electron number effects.[1–9] In this device, a small superconducting island is weakly coupled to a bias circuit through two small-capacitance tunnel junctions and a capacitive gate [Fig. 1(a) inset]. The gate charge $Q_0 = C_g V_g$ controls the most probable number of electrons on the island. Two important energies in this system are the superconducting gap Δ and the characteristic charging energy $E_C = e^2/2C_\Sigma$, where $C_\Sigma = C_1 + C_2 + C_g$ is the total capacitance of the island. These energies typically correspond to microwave frequencies of 10–100 GHz. In very recent work, Kouwenhoven *et al.* demonstrated photon-assisted tunneling (PAT) through a semiconductor quantum dot.[10] In the present paper, we show that when the SET transistor island is *superconducting*, PAT has different and quite dramatic effects. We discuss the mechanism by which the SET transistor with a superconducting island is a sensitive microwave detector, and show that the features that arise in the presence of microwave radiation can be understood quantitatively.

We primarily consider normal-metal–superconductor–normal-metal (*NSN*) SET transistors, devices in which normal-metal Au leads are coupled to the small (30 nm thick by 70 nm wide by 2.2 μm long) superconducting Al island through two $\approx(70\ \text{nm})^2$ AlO_x tunnel junctions. These samples are fabricated as discussed in Ref. 5. For the samples considered in this paper, $E_C \approx 100\ \mu$eV (corresponding to $C_\Sigma \approx 800$ aF), $\Delta \approx 245\ \mu$eV, and the measured tunneling resistances at high bias voltage V are $\approx 100\ \text{k}\Omega$. The samples are measured in a top-loading dilution refrigerator. All sample leads are carefully filtered with conventional low-pass RC filters at room temperature and at the mixing chamber temperature T_{MC}. Each lead also runs for about 30 cm through a Cu-powder ($\sim 10\ \mu$m particle size) microwave filter which is thermally anchored to the mixing chamber. The sample is protected from relatively warm (≈ 4 K) surfaces in the interior of the cryostat by 700 mK and 150 mK Cu shields. However, both shields have an ≈ 1.5 cm circular hole through which a slug containing the sample is top-loaded, so this shielding is incomplete at microwave frequencies and above. Our commercial slug provides significant cold shielding for the sample, but there are mm-scale gaps in this shielding. The experimental data (shown below) indicate that when these gaps are completely covered with conducting material, the sample is protected from microwaves. If the gaps are not completely covered (as in a previous experiment[5]), then small amounts of blackbody radiation from ≈ 4 K surfaces of the cryostat can penetrate the shielding layers and couple to the sample through its leads. In this paper, we present data taken with the gaps in the slug shielding left uncovered (the "incomplete-shielding" case), partially covered (the "better-shielding" case), and completely covered (the "good-shielding" case).

In order to describe the effects of microwave radiation,

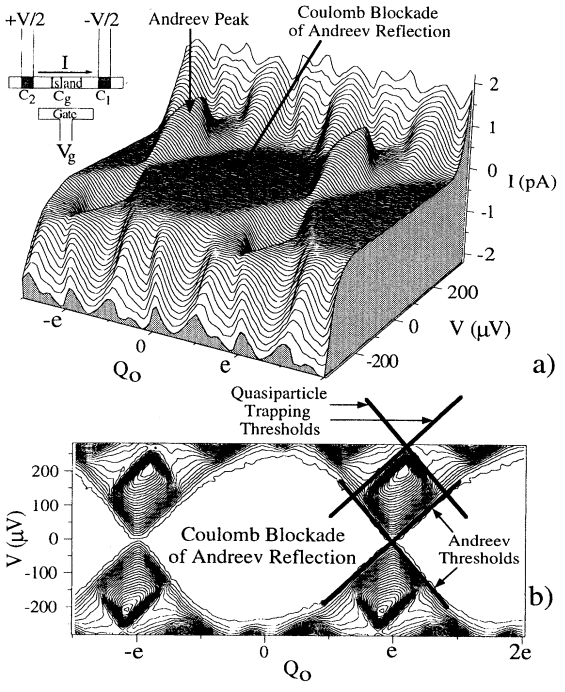

FIG. 1. (a) Experimental "good-shielding" $I(V,Q_0)$ surface for $T_{MC} = 50$ mK showing the $2e$-periodic Andreev peaks and the Coulomb blockade of Andreev reflection. Inset: Schematic diagram of the SET transistor. (b) Contour plot of the same data showing the thresholds for Andreev reflection at each junction, a distinct Coulomb blockade of Andreev reflection, and the quasiparticle trapping thresholds. The contour interval is 40 fA.

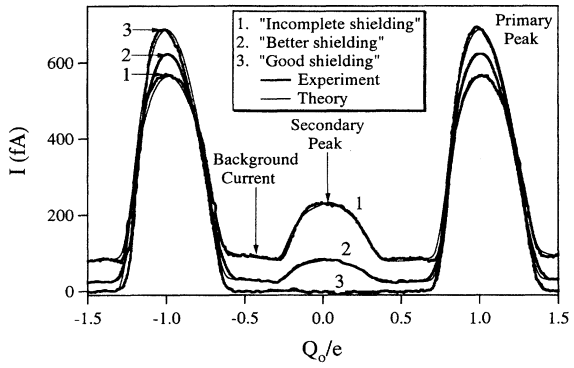

FIG. 2. Three experimental I-Q_0 curves for $V=125$ μV and $T_{MC}=15$ mK for different levels of electromagnetic shielding of the sample. A striking secondary peak near $Q_0=0$ and a nonzero background current appear as the shielding is degraded. Theoretical results (thin lines) for $T_{env}=4$ K and $\alpha R_{env}=0.99$ Ω, 0.19 Ω, and 0 Ω almost perfectly coincide with the incomplete-shielding, better-shielding, and good-shielding data, respectively.

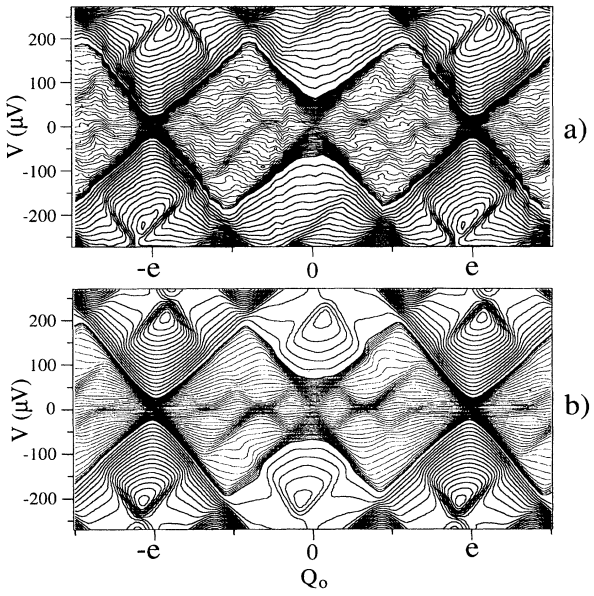

FIG. 3. (a) Contour plot of experimental incomplete-shielding $I(V,Q_0)$ data for $T_{MC}=15$ mK designed to emphasize features within the blockade region. The thinner contours near $V=0$ are spaced at 5 fA intervals, while the slightly thicker contours at higher V are spaced at 40 fA intervals. These thicker contours are drawn only for $|I|\geq 120$ fA. The data exhibit small steps within the blockade region which line up with the quasiparticle trapping thresholds. (b) Corresponding theoretical contour plot for $T_{env}=4$ K and $\alpha R_{env}=0.99$ Ω, the parameters of the incomplete-shielding theory curve of Fig. 2.

we briefly review charge transport in a well-shielded *NSN* SET transistor. In the devices that we consider, $\Delta > E_C$, so that at low V and T the island always contains an even number of conduction electrons.[3–5] Under these conditions, charge transport is dominated by Andreev reflections (two-electron tunneling events) which maintain the even parity of the island. The measured current I through the device as a function of both V and Q_0 is illustrated in Fig. 1(a) for the good-shielding case. The current peaks near $Q_0=\pm e$ result from an Andreev cycle which consists of sequential Andreev reflections at each of the two tunnel junctions.[3–5] As shown in Fig. 1(b), a contour plot of the same well-shielded experimental data, I decreases rapidly at linear thresholds in the V-Q_0 plane.[5,6] At voltages above these thresholds it is energetically favorable for a single electron to tunnel onto the island, changing the island parity from even to odd. Once the electron enters the island, it remains trapped there[4,5] as a quasiparticle for a relatively long time (~ 1 μs),[6] blocking the Andreev cycle. Consequently, I decreases rapidly as V increases through one of these thresholds.

In the good-shielding data of Fig. 1, the Andreev peaks are separated by a region in which the current is zero within the 5 fA current sensitivity of our measurement. This is the region of the Coulomb blockade of Andreev reflection. A slice through the surface of Fig. 1(a) at $V=125$ μV is shown as the good-shielding I-Q_0 curve of Fig. 2. This experimental curve is fit extremely well by the theory of sequential Andreev reflection[4] without including PAT. For this reason, we believe that the good-shielding data are free from measurable effects of microwave radiation.

If we degrade the shielding of the device, microwave irradiation leads to new features in the experimental data. Figure 2 shows how these features emerge as the shielding is degraded. As the amount of absorbed radiation increases, the following changes occur: (1) the primary Andreev peaks [the large ones near $Q_0=(2j+1)e$, j an integer] decrease in size, (2) striking "secondary" peaks near $Q_0=2je$ emerge and grow, and (3) the Coulomb-blockade region develops a nonzero conductance, producing a nonzero background current in I-Q_0 curves.

An additional effect of microwave radiation becomes visible when the incomplete-shielding experimental data are represented in the $I(V,Q_0)$ contour plot of Fig. 3(a).[11] In the presence of microwaves, small steps ($\lesssim 20$ fA) appear within the Coulomb-blockade region. From the positions of the steps, we can identify them with single-electron transitions in which the system is initially in a high-energy state. Such processes are not observed in the absence of radiation because without PAT, these high-energy initial states have vanishingly small occupation probabilities.

The thermal rounding at the bases of the primary Andreev peaks in Fig. 2 provides a useful measure of the electron temperature T. This rounding is fit well with $T=50\pm 20$ mK *regardless of the level of shielding*, indicating that the photon-induced features are not the result of simple heating. Direct measurements and simulations also show that elevated *electron* temperatures do not produce a secondary peak near $Q_0=0$ in the I-Q_0 curves of *NSN* transistors. Thus, we must consider directly the effects of PAT.

We have calculated the effects of PAT on the current through the *NSN* SET transistor by solving a master equation[12] including the following tunneling processes:[13] (1) Andreev reflections, (2) energetically favorable SET events that put a quasiparticle onto the island, (3) photon-assisted, otherwise energetically unfavorable SET events that put a

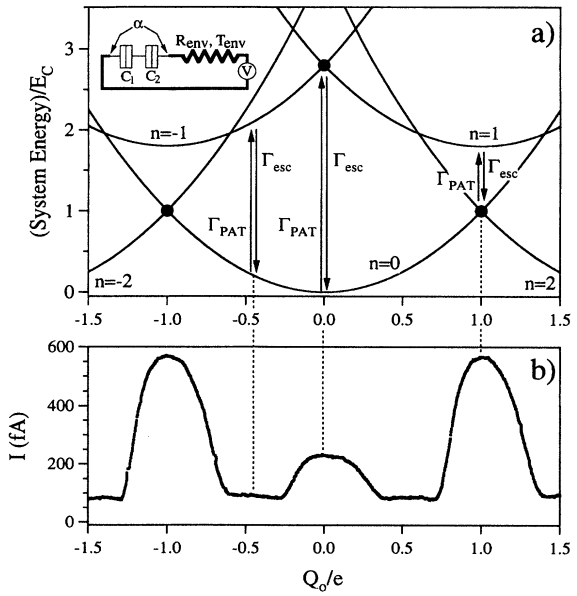

FIG. 4. (a) System energy curves for various charge states drawn for $V=0$ for simplicity. The several pairs of transitions illustrate (from left to right) the origin of the background current, the origin of the secondary peak, and why the primary peaks decrease in size as the amount of absorbed radiation increases. Each pair includes one photon-assisted transition (Γ_{PAT}) and one escape process (Γ_{esc}). The solid circles denote degeneracy points where an Andreev cycle occurs. Inset: Schematic diagram illustrating the model used to account for PAT. (b) Incomplete shielding I-Q_0 curve which illustrates the experimental feature associated with each transition pair of (a).

quasiparticle onto the island, and (4) escape processes in which a quasiparticle is removed from the island.[14] Following Martinis and Nahum,[15] who built upon previous work,[16] we consider radiation from a temperature $T_{env} \gg T$. In this case, PAT greatly enhances the rates of otherwise energetically forbidden tunneling processes. In order to calculate the PAT rates, we take the power spectrum of the voltage fluctuations induced in the bias circuit [Fig. 4(a) inset] by radiation to be a fraction α of the Planck-Nyquist spectrum that would be generated in the high-frequency impedance R_{env} ($\sim 100\ \Omega$) of the one-dimensional leads if they were in equilibrium at the temperature T_{env} (≈ 4 K) of the warm part of the environment. The factor α ($\ll 1$) reflects the weak coupling between the warm region and the sample leads because of shielding. This prescription is mathematically equivalent to using the thermal noise voltage from a resistance αR_{env} at T_{env} in Eq. (3) of Ref. 15 to numerically determine the probability $P(-E)$ that the electromagnetic environment of the device will contribute energy E to a photon-assisted transition.[17] (This sign convention for E follows the definition in Refs. 15 and 16.) With $P(-E)$ in hand we determine all PAT rates using Eq. (1) of Ref. 15.

The thin lines of Fig. 2 are I-Q_0 curves calculated in this way. These theory curves correspond to $T_{env}=4$ K (Ref. 18) and $T=50$ mK, using independently measured junction capacitances and conductances. There is excellent agreement between theory and data in the level of the background current and in the heights and shapes of the primary and secondary peaks. The only difference among the theory curves of Fig. 2 is that the values of αR_{env} used (0.99 Ω, 0.19 Ω, and 0) are changed to reflect the level of shielding.

Figure 3(b) is a contour plot of $I(V,Q_0)$ calculated using the same parameters as the incomplete-shielding curve of Fig. 2. This theoretical plot captures many features of the associated experimental data of Fig. 3(a), including the size and shape of the secondary peak as well as the positions and approximate magnitudes of the small steps within the blockade region. The excellent agreement between theory and experiment shown in Figs. 2 and 3 indicates that PAT in this system is well understood.

The experimental features due to PAT originate as follows. Figure 4(a) shows the system energy for different values of n, the number of excess electrons on the island. The charging energy term $(-en+Q_0)^2/2C_\Sigma$ in the system energy leads to a parabolic shape for each curve. For odd n, the island contains exactly one quasiparticle of energy Δ at low T.[19] To reflect this energy cost, the odd-n parabolas have been shifted upward by Δ ($\approx 2E_C$ for this sample). At the $n=0/n=2$ degeneracy point ($Q_0=e$), current flows due to the Andreev cycle. PAT allows transitions into the $n=1$ state. Consequently, the system spends a smaller fraction of its time at the degeneracy point where the Andreev cycle is possible, leading to reduced current in the primary peak.

The nonzero conductance within the Coulomb-blockade region, and thus the background current, result from PAT across one junction and an escape process across the other [see transitions near $Q_0=-e/2$ in Fig. 4(a)]. Note that PAT can also produce a similar nonzero low-bias conductance in quantum dot systems[10] and in double-junction systems with a *normal-metal* island. This conductance may interfere with the study of elastic cotunneling.[20]

The most dramatic effect of PAT, the secondary peak near $Q_0=0$, is directly linked to superconductivity in the island. It results when PAT introduces a single quasiparticle to the island,[21] a process which is otherwise forbidden at the low V and T considered here. This takes the system from $n=0$ to the $n=\pm 1$ degeneracy point, where current flows by means of the Andreev cycle. The Andreev current continues until the single quasiparticle escapes from the island after a relatively long time of order 1 μs.[6] Consequently, the effect of PAT is magnified because many electrons tunnel through the system for each absorbed photon. In the data of Fig. 4(b), the

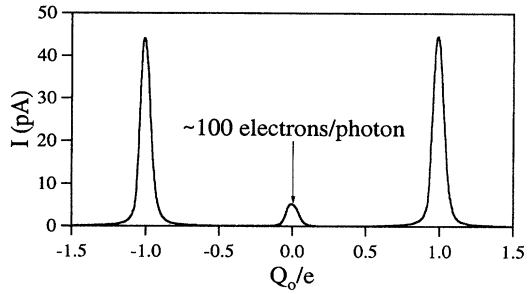

FIG. 5. Experimental incomplete-shielding I-Q_0 curve for an *SSS* SET transistor at $V=20$ μV and $T_{MC}=15$ mK. Near $Q_0=0$ the device acts as a photon-activated switch. The resulting secondary peak corresponds to the tunneling of many electrons for every absorbed photon.

secondary peak corresponds to ≈ 3 electrons tunneling through the system per absorbed photon. This allows a microwave detection scheme in which the height of the secondary peak provides a direct measure of the absorbed power. As a microwave detector, the SET transistor with a superconducting island exceeds the "quantum limit" of one electron per absorbed photon because the photon-assisted transition merely switches the detector current on.

If one considers an all-superconducting (*SSS*) SET transistor, then the small Andreev currents of the *NSN* device (≈ 1 pA) are replaced by much larger (up to ~ 1 nA) supercurrents. This greatly magnifies the secondary peak and increases the microwave sensitivity of the device. Figure 5 shows an experimental I-Q_0 curve for an *SSS* SET transistor taken in the incomplete-shielding case. Note that although the background current is negligible, the secondary peak is quite significant—in this particular device it corresponds to ~ 100 electrons tunneling through the system per absorbed photon. In an optimal *SSS* sample the secondary peak would correspond to as many as $(1\text{ nA})\times(1\ \mu\text{s})/e \sim 10^4$ electrons tunneling per absorbed photon.

In conclusion, we have shown that PAT has dramatic effects in the SET transistor with a superconducting island. It produces a secondary I-Q_0 peak which can be conspicuous in the presence of even every small amounts of microwave radiation because each absorbed photon allows many electrons to tunnel through the system. PAT also produces a nonzero conductance and small steps within the Coulomb-blockade region. All of these experimental features are quantitatively described by a simple model. The SET transistor with a superconducting island is an extremely sensitive microwave detector because it acts as a photon-activated switch.

The authors wish to thank G. Schön, A. Zaikin, J. Siewert, J. Martinis, T. Eiles, K. Likharev, and M. Nahum for valuable input. We also thank C. Black and R. Fitzgerald for their assistance. This work was supported in part by JSEP Grant No. N00014-89-J-1023, ONR Grant No. N-00014-89-J-1565, and NSF Grant No. DMR-92-07956.

---

*Present address: Department of Physics and Astronomy, University of Massachusetts, Amherst, MA 01003.

[1] D. V. Averin and Yu. V. Nazarov, Phys. Rev. Lett. **69**, 1993 (1992).

[2] M. T. Tuominen *et al.*, Phys. Rev. Lett. **69**, 1997 (1992).

[3] T. M. Eiles, J. M. Martinis, and M. H. Devoret, Phys. Rev. Lett. **70**, 1862 (1993).

[4] F. W. J. Hekking *et al.*, Phys. Rev. Lett. **70**, 4138 (1993).

[5] J. M. Hergenrother, M. T. Tuominen, and M. Tinkham, Phys. Rev. Lett. **72**, 1742 (1994).

[6] J. M. Hergenrother *et al.*, Physica B **203**, 327 (1994).

[7] G. Schön and A. D. Zaikin, Europhys. Lett. **26**, 695 (1994).

[8] P. Joyez *et al.*, Phys. Rev. Lett. **72**, 2458 (1994).

[9] A. Amar *et al.*, Phys. Rev. Lett. **72**, 3234 (1994).

[10] L. P. Kouwenhoven *et al.*, Phys. Rev. Lett. **73**, 3443 (1994); L. P. Kouwenhoven *et al.*, Phys. Rev. B **50**, 2019 (1994).

[11] The surface corresponding to this contour plot can be found in Fig. 3(a) of Ref. 5.

[12] D. V. Averin and K. K. Likharev, in *Mesoscopic Phenomena in Solids*, edited by B. Al'tshuler, P. Lee, and R. Webb (Elsevier, Amsterdam, 1991), p. 173.

[13] We ignore cotunneling since it should lead to currents <1 fA for the voltages considered here (Ref. 1).

[14] We assume that the escape processes occur with the rate calculated in Ref. 7.

[15] J. M. Martinis and M. Nahum, Phys. Rev. B **48**, 18 316 (1993).

[16] Yu. V. Nazarov, Zh. Eksp. Teor. Fiz. **95**, 975 (1989) [Sov. Phys. JETP **68**, 561 (1989)]; M. H. Devoret *et al.*, Phys. Rev. Lett. **64**, 1824 (1990); S. M. Girvin *et al.*, *ibid.* **64**, 3183 (1990).

[17] For the relatively high T_{env}'s considered here, we assume that $P(-E)\approx P_T(-E)$, where P_T is the contribution to P due to thermal fluctuations (Ref. 15).

[18] We do not expect the radiation incident on the sample to have a true blackbody spectrum because it originates from surfaces at different temperatures. However, $T_{\text{env}}=4$ K is quite reasonable because the warmest surfaces that radiate into the inner vacuum chamber of our cryostat are at this temperature. Although the data are best fit with $T_{\text{env}}\approx 4$ K, they can be fit reasonably well with any $T_{\text{env}}\gtrsim 3$ K provided that αR_{env} is scaled approximately as $1/T_{\text{env}}^2$. This scaling corresponds to constant total power input, since Stefan's law in one dimension gives a T^2 dependence for radiated power.

[19] We assume for simplicity that n is odd when the total number of conduction electrons on the island is odd.

[20] A. Hanna, M. T. Tuominen, and M. Tinkham, Phys. Rev. Lett. **68**, 3228 (1992).

[21] For the sample of Figs. 1–4 (at low V), this requires a photon of frequency ≈ 80 GHz or higher.